



HAL
open science

Underground Research Laboratories for conducting fault activation experiments in shales.

Yves Guglielmi, Pierre Henry, Christophe Nussbaum, Pierre Dick, Claude Gout, Florian Amann

► **To cite this version:**

Yves Guglielmi, Pierre Henry, Christophe Nussbaum, Pierre Dick, Claude Gout, et al.. Underground Research Laboratories for conducting fault activation experiments in shales.. American Rock Mechanics Association, ARMA, Jun 2015, SAN FRANCISCO, United States. hal-02866935

HAL Id: hal-02866935

<https://hal.science/hal-02866935>

Submitted on 15 Dec 2020

HAL is a multi-disciplinary open access archive for the deposit and dissemination of scientific research documents, whether they are published or not. The documents may come from teaching and research institutions in France or abroad, or from public or private research centers.

L'archive ouverte pluridisciplinaire **HAL**, est destinée au dépôt et à la diffusion de documents scientifiques de niveau recherche, publiés ou non, émanant des établissements d'enseignement et de recherche français ou étrangers, des laboratoires publics ou privés.

Copyright

Underground Research Laboratories for conducting fault activation experiments in shales

Guglielmi, Y.G. and Henry, P.

CEREGE (UMR7330), Aix-Marseille University, CNRS-IRD, 13330 Marseille, France

Nussbaum, C.

Swisstopo, Swiss Geological Survey, Wabern, Switzerland.

Dick, P.

IRSN/PRP-DGE/SRTG, Laboratoire d'Etude et de recherche sur les Transferts et les Interactions dans les Sols, BP 17, 92262 Fontenay-aux-Roses Cedex

Gout, C.

TOTAL S.A., Exploration Production Research and Development, Avenue Larribau – 64018 Pau Cedex – France

Amann, F.

Swiss Competence Center for Energy Research, Earth Science Department, ETH Zurich

Copyright 2015 ARMA, American Rock Mechanics Association

This paper was prepared for presentation at the 49th US Rock Mechanics / Geomechanics Symposium held in San Francisco, CA, USA, 28 June-1 July 2015.

This paper was selected for presentation at the symposium by an ARMA Technical Program Committee based on a technical and critical review of the paper by a minimum of two technical reviewers. The material, as presented, does not necessarily reflect any position of ARMA, its officers, or members. Electronic reproduction, distribution, or storage of any part of this paper for commercial purposes without the written consent of ARMA is prohibited. Permission to reproduce in print is restricted to an abstract of not more than 200 words; illustrations may not be copied. The abstract must contain conspicuous acknowledgement of where and by whom the paper was presented.

ABSTRACT: Since a decade, observations and experiments conducted in underground environments worldwide (mines, underground research laboratories - URL) allowed to bridge the scale gap between laboratory scale and large scale faults. This is particularly important in the study of faults affecting clay formations which could not be observed at the Earth's surface because of weathering processes. Here we show how examples from the Mont Terri (Switzerland) and Tournemire (France) URLs may help in (i) defining the concepts of fault architecture in shales, and (ii) estimating fault hydromechanical properties from decameter scale field experiments. Some key results are that critically stressed shale faults can be reactivated with little stress changes in the range of those produced by shallow underground excavations, and that micrometer-to-millimeter scale reactivations may lead to an increased permeability of one order of magnitude without generating any noticeable seismicity. This appears to be related to complex multi-scale geological processes linked to fault history such as differential hardening, partial sealing, pressure solution and gouge development within the fault zones rather than to the regional state of stress. Such results are important in evaluating fault seal integrity in oil and gas exploration, production or CO₂ storage or monitoring underground excavations for deep geological repositories.

1. INTRODUCTION

Little is known about the rock mechanical characteristics of pre-existing tectonic faults and their influence on rock mass properties and behavior in clay rocks. Underground research laboratories provide exceptional conditions to observe unaltered fault zones in shales and to perform relatively well constrained experiments. Studies on induced macroscopic fracturing around tunnels in faulted shale indicate that reactivation of tectonic faults as a consequence of excavation-induced stress redistributions play an essential role in the development of the Excavation Damage Zone (EDZ) fracture network [1-4]. Hence, faults significantly alter the homogeneity of the rock mass in strength, stress and deformability, and thus have a significant effect on induced fracturing.

Another key point of interest is to evaluate the occurrence and processes controlling radionuclide or fluid (water, hydrocarbons, CO₂) migration through the host rock, from the disposal system to the biosphere or out of the trap. Studies show that if fluid circulations in the undisturbed matrix are very slow (hydraulic conductivity of 10⁻¹⁴ to 10⁻¹⁵ m.s⁻¹), the occurrence of clay-rich fault zones significantly enhance fluid circulation [5]. Here we focus on two fault zones respectively affecting the Upper Toarcian shales at the Institut for Radiological protection and Nuclear Safety (IRSN) Underground Research Laboratory (URL) of Tournemire (Aveyron, France) and the Upper Toarcian-Aalenian Opalinus Clay in the Mont Terri Underground Rock Laboratory (St. Ursanne, Switzerland). We discuss some key architectural, stress and permeability

characters of the two fault zones through the synthesis of different studies conducted at the two sites.

2. FAULT GEOLOGY

The Tournemire Laboratory is located 250m below ground surface in a monoclinic structure composed of three major stratigraphic units: a 250 m thick clay formation (Toarcian-Domerian) intercalated between 200m thick outcropping carbonate deposits of Bathonien-Bajocian-Aalenian and underlying Carixian-Sinemurian carbonates. The studied fault intersects the Toarcian shale formation being part of a complex km-scale fault network [6]. The Mont Terri Laboratory is located in the southern limb of the SW-NE trending Mont Terri anticline which is a flat-ramp-flat structure thrust towards the NW (fault-bend fold) and where the studied fault, although called the “Main Fault” because it is the most deformed zone intersected by the laboratory facilities, is a minor splay (third order structure) of the thrust crossing the Opalinus clay formation, 300m below surface [3]. Both laboratories are dedicated to the study of the thermo-hydro-mechanical integrity of clay formations for application to the storage of nuclear deposits. The Tournemire shale is characterized by a low porosity (8-10 %) with a water content of 3-4% [7, 8] while the Mont Terri shale is characterized by a high porosity (12-18 %) and a water content of 7-8 % [9, 10].

The Tournemire Fault is a N05°-70-to-80°W anticlockwise strike slip fault crossing 0-to-10°N dipping Toarcian shale (Fig.1a-b). This sinistral component on the fault is indeed the last observed movement in the recent stress field, however the main movement was clockwise [11]. The fault zone has been intersected by several boreholes and outcrops in the URL’s galleries walls (Fig.1b). It is about 8-to-10 m thick with a 0.85-to-2.4 m thick anastomosing fault core (FC) and a dissymmetric fractured damage (FDZ) zone 2-to-3 times thicker in the western fault compartment than in the eastern one. Three families of fractures and faults affect the FDZ; respectively N110-to-140, 50°N-or-S, N160, 20-to-40W and N0-to-10, 70-to-80°W. The two first families display large calcite fillings while the third one is characterized by lustrated striated planes that may eventually contain thin gouge material. The fault core displays a high heterogeneity characterized by cataclastic zones of varying thicknesses from 0.4 to 0.01m intercalated with thin 0.1-to-0.2m highly fractured zones (Fig.1b). In the cataclastic zones, shale clasts are bounded/coated by thin (0.001m) clay layers. In the highly fractured zones, most of the fractures are sealed with calcite. At the meter scale, contacts between breccia and highly fractured zones correspond to sliding surfaces. Relatively thick calcite veins are observed at

the FDZ-FC boundary, and the FC calcite bulk content is lower than FDZ’s, respectively of 5 and 10%. Outside the fault zone, the Toarcian shale is almost unfractured. The complex fault zone architecture is related to multi-phase activations of the fault under two main tectonic stress regimes: normal faulting during Upper Jurassic to Lower Cretaceous [12, 13] followed by sinistral strike slip reactivation during the Eocene– Pyrenean compression.

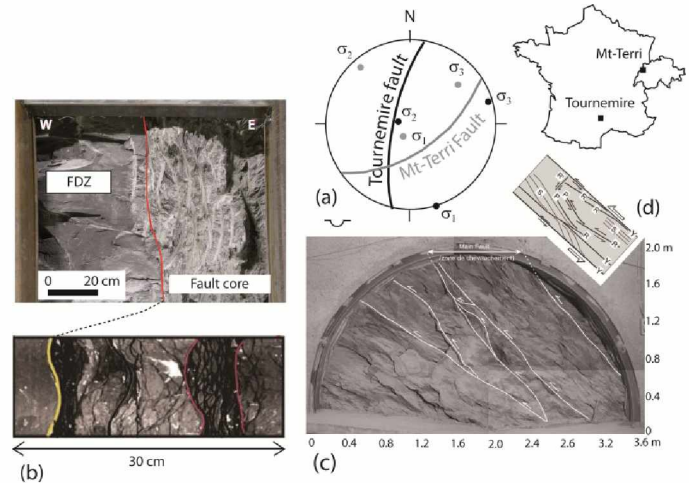


Fig. 1. (a) Stereographic projection of the main fault planes and state of principal stresses (dark is Tournemire, grey is Mont Terri); (b) Fault core-damage zone boundary (red line) outcropping in the Tournemire gallery wall and CT-scanned view of the same boundary (yellow line) on a core of the borehole intersecting the fault. Core shows thin black zones with reoriented clay material that alternate with brecciated (cataclastic) zones; (c) Main Fault outcropping in the Mont Terri gallery wall and (d) Riedel faults network conceptual model of Mont Terri fault core.

The Mont Terri Main Fault consists of a highly deformed zone of about 0.8-to-3m width composed of a complex network of single faults and scaly clays (Figure 1c). Around this thrust zone, the galleries are cut by many faults and fractures associated to the same deformation regime. Compared to Tournemire, what is called the “Main Fault” could correspond to Tournemire’s fault core, the damaged zone being, in Mont Terri, much more extended or “hidden” by other satellite fault zones. Indeed, an increase in the fault density was observed close to the “Main fault” while boundaries of the FDZ are unclear. In the tunnel, the Main Fault plunges to the SE with a mean dip of about 50° and intersects the stratification which gently dips 35° to the SE. The detailed fracture network visible at the outcrop scale and strain intensity within the zone of the Main Fault is heterogeneous [3], characterized, as in Tournemire’s FC, by zones with fault gouge, C’-type shear bands, meso-scale folds, micro-folds, numerous fault planes and apparently undisturbed parts (Figure 1c). Parts of the Main Fault comprise a ‘scaly’ fabric [14], where the rock splits progressively into smaller

fish-like flakes. The different sets of faults in the Main Fault can be interpreted as Riedel P- and R-shears (Fig.2e). The Main Fault can be interpreted as a shear fault-bend fold [3], which was passively steepened from 20° to the range of 40°-45° in sequence with the folding of the Mont Terri anticline over a basal ramp during the folding of the Jura belt in late Miocene. The offset of the Main Fault is inferred to be relatively small (~10 m) but difficult to determine precisely in absence of reliable markers. The Main Fault is an aborted blind thrust and is interpreted to be an internal thrust within the Opalinus Clay, soling at the base of the Opalinus Clay formation. The kinematics of the Main Fault have been inferred by paleostress analysis of slickenlines, showing σ_1 to be sub-horizontal, trending NNW-SSE for a reverse faulting mode [3]. This geometry agrees with the “distant push” or “Fernschub” theory of the Jura folding as a consequence of the propagation of the Alpine foreland towards NNW [15]. Kinematic criteria support the thrust movement towards the NNW with a slight dextral component. A second generation of oblique slickenlines attests that part of the deformation was probably not plane strain. P-T conditions at the time of the onset of motion of the Main Fault are inferred by [16] to be about 55°C under an overburden of maximum 1000 m. In comparison, the P-T conditions of the Tournemire fault was 110° C under an overburden of 2.5 km [17].

The two studied faults show common architectural characteristics defined by a decameter thick fractured damage zone and a complex 1-to-2m thick fault core where meter scale Riedel planes bound cataclastic and/or highly fractured lenses. In the fault core, thin clay layers are observed in the Riedel planes or between the clasts in the cataclastic lenses showing that a reorganization of the clay minerals occurs during shear deformation. FDZ fractures are more or less sealed with calcite, and a decrease of the calcite content is observed in the FC.

3. FAULT STRENGTH/STRESS PROPERTIES

The in-situ stress state at the level of the Mont Terri URL was estimated by [18] using three-dimensional numerical modeling and field data from stress-induced borehole breakouts and different stress measurement methods in the shale facies (Fig.1a). Their analyses suggest a sub-vertical maximum principal stress direction which is steeply (70°) inclined towards SSW with a magnitude of 6.5 MPa, a sub-horizontal intermediate principal stress direction trending with 10° towards NW with a magnitude of 4 MPa, and a sub-horizontal minimum principal stress direction trending towards NE with a magnitude of 0.6-to-2.9 MPa (Fig. 1a). During the excavation of a gallery across the Main Fault, excavation-induced displacements of the gallery

wall and deformations of natural pre-existing faults were continuously monitored [4].

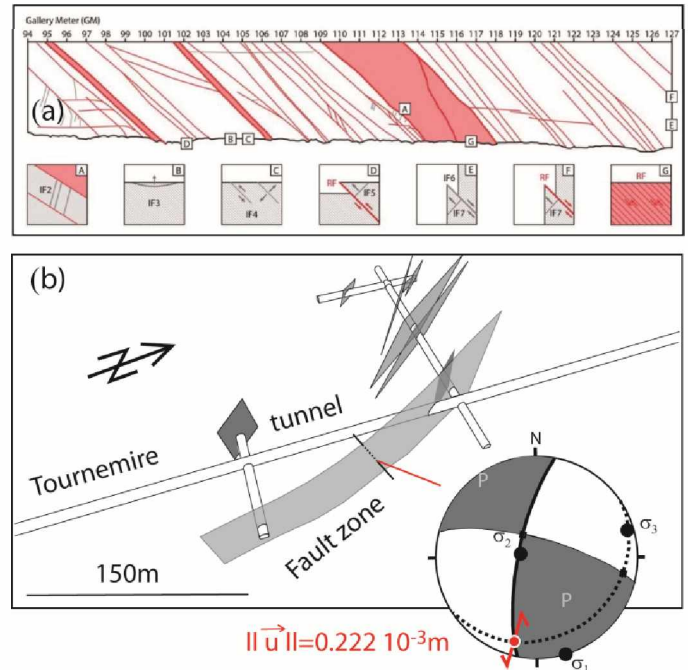


Fig. 2. (a) – Conceptual model of [19] which illustrates the generalized structural and kinematic relationships between pre-existing tectonic faults (RF) and excavation-induced fractures (IF) around the Mont Terri gallery intersecting the Main Fault (bedding is in grey dotted lines parallel to the SSE-dipping faults (red lines), excavation induced fractures are shown by grey lines); (b) - Slip vector orientation and modulus measured above the fault opening pressure point (FP) when activating the Tournemire fault. We used the dihedral method [20] to determine the compression P and tension T zones between the fault plane and the auxiliary plane.

Data revealed that the rock mass response is substantially governed by both the rock anisotropy and the kinematic failure of individual fault planes. Fault plane reactivations mainly occurred at the tunnel face (Figure 2a), crown and the invert, and less in the sidewalls and at larger depths in the rock mass, respectively, because of the unfavorable orientation of the planes towards excavation induced stress perturbations and the attenuation of the excavation induced stress magnitude perturbation. The rock mass response was dominated by extensional fracturing through the intact rock matrix resulting in large displacements (up to 40 mm) adjacent to fault zones. Considering a bilinear Mohr-Coulomb failure criterion deduced from direct shear laboratory tests on fault planes in a three-dimensional finite differences representation of both the gallery and the fault zone geology, [19] calculated that such displacements were induced by a minimum principal stress decrease of about 1 MPa and maximum principal stress increase of about 2 MPa at 0.3m depth from the gallery walls close to the

fault zones. Using about the same state of stresses and fault properties, characterized by a cohesion of 0.2-to-0.6 MPa and a peak static friction angle of 22° , Main Fault slip tendency analyses confirmed that given the Mt Terri's range of pore pressures of about 2 MPa (far from the galleries), the fault is close to a critical state for normal slip and dilation on a varying activated area of 1425 – to – 1460 m².

In Tournemire, the actual state of stresses was determined with a series of leak off tests performed in a vertical 180 m deep borehole located in the intact shale 50 m from the fault zone [20], revealing a strike slip regime at the experiment depth characterized by $\sigma_1 = 4 \pm 2$ MPa, horizontal and oriented $N162^\circ \pm 15^\circ E$, $\sigma_2 = 3.8 \pm 0.4$ MPa, $7-8^\circ$ inclined from vertical in the $N72^\circ$ direction and $\sigma_3 = 2.1 \pm 1$ MPa, $7-8^\circ$ inclined from horizontal in the $N72^\circ$ direction (Figure 1a). An inclined borehole was drilled to intersect the fault zone at a distance of about 10-to-15m from the tunnel where the fault was pressurized using a straddle packer system defining a 2.4 m long injection chamber normal to the fault surface (Fig.3b). Several fault zone intervals were tested in the fault damage zone and in the fault core. A three-dimensional displacement sensor set in the chamber allowed continuous synchronous coupled monitoring of fault movements, injection pressure and flow rate [5]. An anticlockwise 0.05-to-0.22 mm fault slip was captured in good accordance with the orientation of preexisting fault surface towards the principal stresses. Depending on the tests, the fault activation occurred at injection pressures of 1.5-to-3.2 MPa revealing the effects of both a heterogeneity of the stress tensor within the fault zone and strong strength contrasts between the FDZ and the FC characterized by peak static frictions of 34 and 22° and cohesions of 0.5 and 0 MPa respectively.

Experiments conducted in both URLs show similar results given the highly similar principal stress magnitudes but different stress regimes respectively normal in Mt Terri and strike slip in Tournemire. Faults are activated at stress variations that are within the range of the perturbations induced by galleries excavations. The same 22° peak static friction properties of the FC were deduced from laboratory tests and numerical analyses in Mont Terri, and from the field fault activation experiment in Tournemire. In detail, friction values much higher (34°) were obtained in the Tournemire's fault FDZ and same range of cohesion was found. These experiments show that faults may easily reactivate during tunnel excavation if they are favorably oriented in respect to the in-situ state of stress. Reactivation may not be simple since a significant friction contrast appears between the shale fault core and damage zone.

4. FAULT PERMEABILITY VARIATIONS

To assess the transport properties associated with the Tournemire fault, a modular mini-packer system (MMPS) hydraulic testing was conducted in multiple boreholes to characterize hydraulic conductivities within the formation. Pressure data collected during the hydraulic tests were analyzed using the nSIGHTS (n-dimensional Statistical Inverse Graphical Hydraulic Test Simulator) code to estimate hydraulic conductivity and formation pressures of the tested intervals. Preliminary results indicate hydraulic conductivities of $5 \cdot 10^{-12}$ m.s⁻¹ in the fault core and damaged zone, and 10^{-14} m.s⁻¹ in the adjacent undisturbed shale. At Mont Terri, a compilation was done of all data concerning the permeability obtained from hydraulic packer tests performed in different boreholes within the framework of various experiments [21]. The statistical analysis of data shows that the hydraulic conductivities of intact shale and fault zones are ranging between 9×10^{-15} and 6×10^{-12} m.s⁻¹. All these tests were performed at low imposed pressure below 1 MPa, considering that no movement of the fault was occurring.

There are few field data on stress induced hydraulic conductivity variations of clay faults. In the laboratory, low 1-2 MPa effective normal stress variations induced hydraulic conductivity variations of clay fractures may result from a complex combination of clay mineral swelling, consolidation and creep [22, 23]. Some laboratory experiments conducted on Opalinus clay fractures by [24] show that conductivity may decrease initially at low shear strain then increase at high strains through fracture generation out of the main shear plane. Recently, a fault pressurization experiment has been conducted in the core of Tournemire fault (location in Fig.2). Water pressure was increased step-by-step in a straddle packer interval set across the fault core. At each pressure step, pressure was held for a given amount of time (about 250 seconds), then increased to the next step until reaching the fault opening pressure which is when pressure 'break-over' occurs i.e. large increase in flow rate results in small pressure increases. A 300 seconds long constant pressure was then held at a pressure above the fracture opening pressure. Then a step-down procedure was performed until the pressure returned to its initial value.

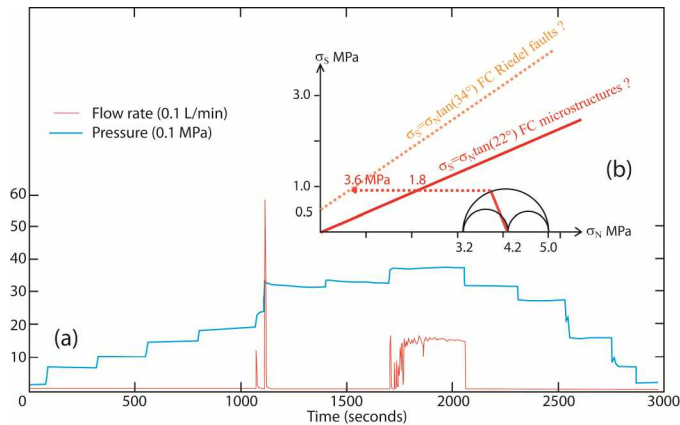


Figure 3: (a) - Pressure and Flow rate time variations during the injection in the Tournemire fault core; (b) - Mohr-Coulomb representation of the strength and state of stresses during the test.

Pressure and flow rate-vs-time curves show a complex fault core leakage activation (Fig.3a) characterized by transient flow rate pulses occurring between 1.5 and 2.2 MPa, followed by a no-leakage period and the progressive transition from transient pulses to quasi-steady state flow at 3.6MPa. Using an analytical pseudo-state solution of the radial diffusivity equation for a relatively incompressible fluid to describe the pressure-versus-flow rate curve above 3.6MPa yields a $10\text{-to-}30 \times 10^{-6} \text{ m.s}^{-1}$ permeability value at fault opening. Below 3.6 MPa, no steady state flow was measured into the fault because of the relatively low sensitivity of the straddle packer apparatus at low injected pressures. Taking the values at low stress given by [23] from tests conducted in the same fault, we conclude that the effective stress variation in the fault induced a five orders of magnitude permeability increase from 5.10^{-12} to $1\text{-to-}3 \times 10^{-7} \text{ m.s}^{-1}$. Interestingly, if we consider the state of stresses in the fault core with strength properties characterized by no cohesion and a peak static friction angle of 22° , we can calculate that this permeability increase should occur at shear failure for a 1.8MPa pressure variation (Figure 3b). This value matches the pressure when the transient pulse of flow rate initiates (at 1.5-to-2.2 MPa in Fig.3a) but does not match the significant quasi-steady-state flow rate regime occurring for injection pressures much higher than the yield point in the Mohr-Coulomb diagram (Figures 4a and b). Such observations highlight that permeability variation of the fault core is related to complex mixed failure modes associated with both the microscopic evolution of fabric elements in clay rich fault gouge and to the macroscopic reactivation of pre-existing discontinuities (potentially the Riedel faults as shown in Fig.3b).

5. CONCLUSIONS

Both underground research laboratories at Tournemire and Mont Terri provide access to unaltered fault zones in shales. Although the geological history of the faults is different, some common architectural characteristics may be observed: a fractured damage zone where many fractures are sealed with calcite and a core zone where intense deformation is characterized by complex mechanisms of cataclasis, clay minerals reorientation and macroscopic scale Riedel planes. It results in a high potential instability of some faults elements to relatively small stress variations within the range of magnitudes of the ones induced by galleries excavation. Such instability is explained by the orientation of fault surfaces to stress and by high contrasts in strength properties characterized by a low peak static friction of the fault core and cohesive sealed-with-calcite fractures of the fault damage zone. Understanding permeability variations related to shale faults activation appears as one of the most promising challenge that can be studied in the URL's. Indeed, permeability tests conducted at pore pressures that cannot induce any fault deformation tend to show relatively reduced contrasts of values between fault and intact shale permeability. Recently, URL facilities allowed one to conduct local supra-hydrostatic pore pressure increases in a fault while many hydrogeophysical parameters were monitored close to the source, showing permeability increase of several orders of magnitude at low strain rates on critically stressed shale faults. These experiments may thus help refine the physics of fluids hydromechanical effects during shale fault reactivation, opening new experimental perspectives to relate these effects to aseismic-to-seismic fault movements.

REFERENCES

1. Bluemling, P. and H. Konietzky. 2003. Development of an excavation disturbed zone in Claystone (Opalinus Clay). *Geotechnical Measurements and Modelling*, Natau, Fecker & Pimentel (eds), Swets & Zeitlinger, Lisse, ISBN 90 5809 603 3.
2. Yong, S. 2008. A three-dimensional analysis of excavation-induced perturbations in the Opalinus Clay at the Mont Terri Rock Laboratory. *PhD thesis*, Department of Earth Sciences. ETH Zurich, Switzerland.
3. Nussbaum, C, P. Bossart, F. Amann, and C. Aubourg. 2011. Analysis of tectonic structures and excavation induced fractures in the Opalinus Clay, Mont Terri underground rock laboratory (Switzerland). *Swiss J Geosci* 104: 187-210.
4. Thoeny, R. 2014. Geomechanical analysis of excavation-induced rock mass behavior of faulted Opalinus Clay at the Mont Terri Underground Rock

- Laboratory (Switzerland). *PhD thesis*, Department of Earth Sciences. ETH Zurich, Switzerland.
5. Guglielmi, Y., F. Cappa, H. Lançon, J.B. Janowczyk, J. Rutqvist, C.F. Tsang, and J.S.Y. Wang. 2013. ISRM Suggested Method for Step-Rate Injection Method for Fracture In-Situ Properties (SIMFIP): Using a 3-Components Borehole Deformation Sensor. *Rock Mech. Rock Eng.*, DOI 10.1007/s00603-013-0517-1.
 6. Dick, P., C. Wittebroodt, M. Lefevre, C. Courbet, and J.M. Matray. 2013. Estimating hydraulic conductivities in a fractured shale formation from pressure pulse testing and 3D modeling. *American Geophysical Union*, Fall Meeting 2013, abstract #MR11A-2202.
 7. Matray, J.M., S. Savoye, and J. Cabrera. 2007. Desaturation and structure relationships around drifts excavated in the well-compacted Tournemire's argillite (Aveyron, France). *Engineering Geology* 90, 1–16.
 8. Constantin, J., J.B. Peyaud, P. Vergély, M. Pagel, and J. Cabrera. 2004. Evolution of the structural fault permeability in argillaceous rocks in a polyphased tectonic context. *Physics and Chemistry of the Earth* 29, 25-41.
 9. Amann F, R. Thoeny, P.K. Kaiser, and E.A. Button. 2011. Insight into the brittle failure behavior of clay shales in unconfined and confined compression, *Proceedings of the 45th US Rock Mechanics/Geomechanics Symposium 2011*, San Francisco, CA, American Rock Mechanics Association, ARMA 11-536
 10. Wymann, L.P. 2013. The influence of saturation on the uniaxial compressive strength of Opalinus Clay. *MSc thesis*, Department of Earth Sciences, ETH Zurich, Switzerland.
 11. Constantin, J. 2002. Fracturation et paléocirculations de fluide dans les formations géologiques de faible perméabilité matricielle : le cas des argilites de Tournemire (Aveyron, France). *PhD Thesis*, University Paris-Sud, 260 p.
 12. Bles, J.L., D. Bonijoly, C. Castaing, and Y. Gros. 1989. Successive post-Variscan stress fields in the French Massif Central and its borders (western European plate): comparison with geodynamic data. *Tectonophysics* 169, 79–111.
 13. Martin, P. and F. Bergerat. 1996. Paleo-stresses inferred from macro- and microfractures in the Balazuc-1 borehole (GPF programme). Contribution to the tectonic evolution of the Cevennes border of the SE Basin of France. *Mar. Pet. Geol.* 6, 671–684.
 14. Laurich, B., J.L.Urai, G. Desbois, C. Vollmer, and C. Nussbaum. 2014. Microstructural evolution of an incipient fault zone in Opalinus Clay: Insights from an optical and electron microscopic study of ion-beam polished samples from the Main Fault in the Mt-Terri Underground Research Laboratory. *J. Struct. Geol.* 67, 107-128, <http://dx.doi.org/10.1016/j.jsg.2014.07.014>
 15. Laubscher, H., 1961. Die Fernschubhypothese der Jurafaltung. *Eclogae Geol. Helv.* 54, 221-280.
 16. Mazurek, M., A.J. Hurford, and W. Leu. 2006. Unravelling the multi-stage burial history of the Swiss Molasse Basin: integration of apatite fission track, vitrinite reflectance and biomarker isomerisation analysis. *Basin Res.* 18, 27e50. <http://dx.doi.org/10.1111/j.1365-2117.2006.00286.x>.
 17. Peyaud, J. B., J. Barbarand, A. Carter, and M. Pagel. 2005. Mid-Cretaceous uplift and erosion on the northern margin of the Ligurian Tethys deduced from thermal history reconstruction, *Int. J. Earth Sci.*, 94, 46247.
 18. Martin C.D. and G.W. Lanyon. 2003. Measurement of in-situ stress in weak rocks at Mont Terri Rock Lab. *International Journal of Rock Mechanics and Mining Sciences*, 40 (7-8):1077-1088.
 19. Angelier, J. 1984. Tectonic analysis of fault slip data sets. *Journal of Geophysical Research* 89 (B7), 5835–5848.
 20. Cornet, F.H. 2000. Détermination du champ de contrainte au voisinage du laboratoire souterrain de Tournemire. *Rapport du Laboratoire de Mécanique des Roches*, Département de Sismologie, Institut de Physique du Globe de Paris, Rapport N°98N33/0073.
 21. Nussbaum, C., and P. Bossart. 2004. Compilation of K-values from packer tests in the Mont Terri rock laboratory. *Technical Note 2005-10*, Mont Terri Project, Switzerland.
 22. Bastiaens, W., F. Bernier, and X.L. Li. 2007. SELFRAC : experiments and conclusions on fracturing, self-healing and self-sealing processes in clays. *Physics and Chemistry of the Earth* 32, 600-615.
 23. Gutierrez, M., L.E. Øinob, and R. Nygardc. 2000. Stress-dependent permeability of a mineralised fracture in shale. *Marine and Petroleum Geology* 17, 895-907.
 24. Cuss, R.J., A. Milodowski, and J.F. Harrington. 2011. Fracture transmissivity as a function of normal and shear stress: First results in Opalinus Clay. *Physics and Chemistry of the Earth* 36, 1960-1971.